

1 **Rapid carbon accumulation at a saltmarsh restored by managed realignment far exceeds carbon
2 emitted in site construction**

3

4 Hannah L. Mossman^{1*}, Nigel Pontee^{2,3}, Katie Born⁴, Peter J. Lawrence^{1,5}, Stuart Rae¹, James Scott⁶,
5 Beatriz Serato², Robert B. Sparkes¹, Martin J.P. Sullivan¹, Rachel M. Dunk¹

6

7 ¹ Ecology and Environment Research Centre, Department of Natural Sciences, Manchester
8 Metropolitan University, Chester Street, Manchester M1 5GD, UK

9 ² Jacobs, 1 The West Wing, 1 Glass Wharf, Bristol, BS2 0EL, UK

10 ³ University of Southampton, Southampton, SO14 3ZH, UK

11 ⁴ Jacobs, 160 Dundee Street, Edinburgh EH11 1DQ, UK

12 ⁵ School of Ocean Sciences, Bangor University, Menai Bridge LL59 5AB, UK

13 ⁶ Jacobs, 1st Floor office, Aperture, Pynes Hill, Rydon Lane, Exeter, EX2 5AZ, UK

14

15 * Corresponding author: Dr Hannah L Mossman, h.mossman@mmu.ac.uk

16

17 **Abstract**

18 Increasing attention is being paid to the carbon sequestration and storage services provided by
19 coastal blue carbon ecosystems such as saltmarshes. Sites restored by managed realignment, where
20 existing sea walls are breached to reinstate tidal inundation to the land behind, have considerable
21 potential to accumulate carbon through deposition of sediment brought in by the tide and burial of
22 vegetation in the site. While this potential has been recognised, it is not yet a common motivating
23 factor for saltmarsh restoration, partly due to uncertainties about the rate of carbon accumulation
24 and how this balances against the greenhouse gases emitted during site construction. We use a
25 combination of field measurements over four years and remote sensing to quantify carbon
26 accumulation at a large managed realignment site, Steart Marshes, UK. Sediment accumulated
27 rapidly at Steart Marshes (mean of 75 mm yr⁻¹) and had a high carbon content (4.4% total carbon,
28 2.2% total organic carbon), resulting in carbon accumulation of 36.6 t ha⁻¹ yr⁻¹ total carbon (19.4 t ha⁻¹
29 yr⁻¹ total organic carbon). This rate of carbon accumulation is an order of magnitude higher than
30 reported in many other restored saltmarshes, and is higher although more similar to values
31 previously reported from another hypertidal system (Bay of Fundy, Canada). The estimated carbon
32 emissions associated with the construction of the site were ~2-4% of the observed carbon
33 accumulation during the study period, supporting the view that managed realignment projects in
34 such settings are likely to have significant carbon accumulation benefits. We outline further
35 considerations that are needed to move towards a full carbon budget for saltmarsh restoration.

36

37 **Keywords:** Blue carbon; salt marsh; nature-based solution

38 **Introduction**

39 Earth's ecosystems exhibit overall net carbon uptake, causing increases in atmospheric CO₂ to be
40 smaller than expected from fossil emissions and land-use change [1]. They also contain substantial
41 carbon stocks, which currently store carbon out of the atmosphere but are sensitive to changes in
42 climate or land-use [2, 3]. Coastal 'blue carbon' ecosystems, including saltmarshes, are especially
43 carbon dense and sequester carbon at a rate an order of magnitude faster than terrestrial
44 ecosystems [4]. Both allochthonous and autochthonous carbon is sequestered in saltmarshes;
45 carbon accumulates in saltmarshes as sediment carried in by the tide is deposited, and this sediment
46 buries saltmarsh plant remains. Globally, the ~5.5 million hectares of saltmarshes [5] are estimated
47 to accumulate carbon at an average rate of ~2.4 t C ha⁻¹ yr⁻¹ [6]. Despite their importance, ~50% of
48 saltmarsh area has been lost, particularly through reclamation for agriculture or urbanisation, or
49 degraded [7], with annual losses of 1-2% [8, 9].

50 In response to losses of saltmarsh and its associated biodiversity, 'no net loss' policies have sought
51 to protect remaining wetlands and create new habitat [10], contributing to over 100,000 ha of
52 intertidal wetland creation over the last 30 years [11]. However, the pace of global wetland creation
53 is not sufficient to offset losses, where a key barrier is the availability of project financing [12].
54 Payments for ecosystem services, such as flood protection or biodiversity, offer potential financial
55 mechanisms for saltmarsh creation or restoration [13]. Carbon accumulation (and thus climate
56 mitigation) has been recognised as a potential benefit of saltmarsh restoration, and could therefore
57 provide a further motivation for site creation [14, 15].

58 Robustly quantifying the rate of carbon accumulation on restored saltmarshes will be necessary if
59 carbon finance mechanisms are to be developed [16] and is also important to enable saltmarsh
60 restoration to be properly included in national carbon budgets [17]. Furthermore, rising sea levels
61 threaten existing saltmarshes, and the climate sensitivity of their carbon stocks and fluxes needs to
62 be quantified [18]. While saltmarsh restoration could potentially compensate for loss of natural
63 saltmarshes, given known differences in topography and ecology [19, 20], it may not be appropriate
64 to assume that restored or created marshes will ultimately store carbon at a rate comparable to
65 natural saltmarshes [21]. Thus it is also important to determine any differences between carbon
66 accumulation and sequestration in natural and restored saltmarsh.

67 Previous attempts to quantify actual or potential carbon accumulation following saltmarsh
68 restoration have used a variety of techniques: (a) spatially explicit models to predict landscape-scale
69 carbon accumulation based on observed carbon accumulation in natural habitats [22]; (b)
70 measurements at a single time-point to take a snapshot of carbon stocks [23]; (c) restored

71 saltmarshes of different ages as a space-for-time substitution to estimate the rate of carbon
72 accumulation [24]; and (d) repeat measurements of the elevation of sediment surface to quantify
73 sediment deposition rates [25]. While all approaches highlight the potential for saltmarsh
74 restoration to lead to carbon accumulation, each has limitations when used in isolation. A further
75 challenge is that previous studies have either assessed only total carbon (which does not distinguish
76 organic carbon from inorganic carbon such as biogenic or lithogenic carbonates), or have quantified
77 organic carbon using loss on ignition, which is known to have poor accuracy and large uncertainties
78 [26].

79 A further consideration when evaluating the net carbon benefit of a saltmarsh restoration or
80 creation project is the balance between the carbon costs of constructing the site (e.g. building new
81 flood defences inland and breaching the existing embankments, termed “managed realignment”)
82 and the carbon accumulation provided by the site [e.g. 27]. If project carbon costs are high relative
83 to the rate of carbon accumulation, it may take years for the site to pay off the debt of construction
84 [28].

85 This research aims to evaluate carbon costs and benefits from saltmarsh creation through managed
86 realignment, using a novel combination of techniques. Over the course of several annual cycles we
87 use remote sensing, field measurements and robust laboratory techniques to quantify total and
88 organic carbon accumulation in an evolving saltmarsh in the first years after restoration. This allows
89 us to reliably quantify the amount and rate of carbon accumulation following restoration. We then
90 assess the carbon emissions incurred during site construction before identifying additional
91 requirements for producing a full carbon budget for saltmarsh restoration.

92

93 **Materials and Methods**

94 Study site

95 Steart Marshes (Somerset, UK; 51.20 N, 3.05 W) is a 250-ha managed realignment site, forming part
96 of a larger 400 ha complex of restored wetland habitats managed by the Wildfowl and Wetlands
97 Trust. It was constructed to create new intertidal habitat in compensation for previous losses, and to
98 provide enhanced flood defences [29]. Prior to site construction, the land was under a mix of
99 agricultural uses, including permanent pasture (i.e. pasture had been the land use over many years),
100 grass ley (part of cyclical arable land management) and arable (winter wheat, barley, oilseed rape
101 and maize) (Fig. 1a). The site lies near the mouth of the River Parrett which drains a catchment of
102 interbedded limestone and mudstone [30] and flows into the Severn Estuary. Hydrodynamic

103 processes in the Parrett are dominated by a large tidal range which gives rise to strong tidal flows
104 and large intertidal areas. At Hinkley, just to the west of the Parrett Estuary mouth, the mean spring
105 tides have a high water height of 5.6 mODN and a low water height of -5.1 mODN, giving a range of
106 approximately 11m [31, 32].

107 The construction of the managed realignment site started in early 2012, comprising the excavation
108 of a creek network and pools, the construction of new flood defence embankments and the raising
109 of a small length of existing embankment. The creek network (7.6 km total length) was designed to
110 meet the geomorphological requirements of the scheme (see [33] for details), aid establishment of
111 intertidal habitat, and minimise material transport distances by enabling construction of the
112 required embankments from the excavated material [29]. In total, 4.75 km of new 4 m high or raised
113 flood defence embankments were constructed (Fig. 1a). All material used in the construction of the
114 new embankments was obtained from the site, i.e. embankments were created from clays
115 excavated from within site and no concrete was used in embankment construction. Several lagoons
116 were excavated to enhance habitat provision for birds and fish, and islands were created from
117 excess material to provide protected roosting and nesting locations for birds at elevations high
118 enough to avoid excessive inundation by the tide [29]. In total, 489,422 m³ of material was
119 excavated and moved within the site during construction. A single, 250 m wide breach in the sea
120 wall was created in September 2014, allowing regular tidal inundation to occur (further details of the
121 breach are provided in [31]).

122

123 Field sampling design

124 Four areas of the site were selected for regular sampling, first an area substantially disturbed by
125 earth moving vehicles during construction (Site A, Fig. 1a) and three sites based on prior land use,
126 permanent pasture (Site B), grass ley (Site C) and arable (Site D). Within these areas, we selected
127 three sampling locations, stratified by the elevation prior to restoration of tidal inundation; the area
128 of permanent pasture was relatively homogenous in elevation and so we only selected two sampling
129 sites. To act as a natural reference, we selected a neighbouring area of pioneer saltmarsh (mostly
130 bare ground with some *Spartina anglica*) and an area of saltmarsh with plant communities similar to
131 those anticipated to establish on the managed realignment site, i.e. those dominated by *Puccinellia*
132 *maritima* and *Aster tripolium* (NAT, Fig. 1a). This gave a total of thirteen regular sampling locations
133 within five sampling sites.

134

135 Sediment collection, preparation and storage

136 Sediments were sampled at each location immediately prior to restoration (28 August 2014, Sites A-
137 D but not natural marsh), in December 2014 and then once or twice annually in 2015, 2016 and
138 2017, giving one pre-restoration and six post-restoration sampling time points (see Table S1 for full
139 details). Cores of 30-50cm were collected using a soil auger and sectioned into 5-10 cm lengths for
140 later analysis. In total, we collected 78 cores, resulting in 596 samples. Depending on site conditions,
141 surface silts deposited post-breach were sometimes difficult to sample using a soil auger as they
142 were either prone to compression or highly friable. In these cases, we collected undisturbed surface
143 samples using adapted syringe tubes and/or collected the full surface sediment plates (down to base
144 of mud cracks), and then sampled deeper sediments by taking a core between mud cracks. The
145 horizon between the deposited silts and the underlying agricultural soils was determined through
146 visual inspection of the cores (prior to sub-sampling) and the depth (in core and from surface) was
147 recorded. The horizon was readily identifiable through a change in colour and texture of the soils,
148 and by the presence of remnant vegetation and roots. Samples with a defined volume of 5 cm³ were
149 taken from the above-horizon section of the core or directly from surface sediments for dry bulk
150 density measurements [34].

151 All samples were stored at 4°C prior to analysis. Dry bulk density was determined by drying the
152 samples of a known volume to a constant weight at 105°C. The remaining core samples were dried
153 at 60°C, covered, in aluminium trays/glass jars for approximately 96 hours, then ground using a
154 pestle and mortar to ensure a homogeneous sample for further analysis.

155

156 Quantifying carbon composition of the sediment

157 We quantified the total carbon (TC) in all core sections collected. Total carbon contents were
158 measured on dried, ground sediment samples using elemental analysis (LECO CR-412 Carbon
159 Analyser (LECO Corporation, MI, USA) and Vario EL Cube (Elementar, Germany) instruments).
160 Certified Reference Materials were analysed on both instruments and replicates of an internal
161 standard (bulk sample of surface sediments collected from the site) were included in all instrument
162 runs. The measured carbon content of the CRM on the LECO instrument was consistently higher
163 than the certified value (Leco Soil Standard 502-062 (n=42), measured %C = 2.12±0.02, certified %C =
164 2.01±0.03), while analysis of the CRM on the Elementar instrument showed excellent agreement
165 (Elemental Microanalysis Ltd Soil Standard B2184 (n=6), measured %C = 2.29±0.06, certified %C =
166 2.31±0.06). Accordingly, all LECO measurements were multiplied by a correction factor of 0.95

167 (2.01/2.12). The corrected analysis of the internal standard on the LECO instrument showed
168 excellent agreement with the Elementar analysis (LECO (n=83), %C = 2.74±0.10; Elementar (n=18),
169 %C = 2.68±0.11)..

170 To quantify total organic carbon (TOC), we selected one core from each site (A-D and NAT) from the
171 most recent sampling period; for the restored marsh (sites A-D), TOC was quantified on the newly
172 accreted sediment (above horizon) only. These samples underwent acid digestion to remove
173 inorganic carbon. Excess 1N HCl was added, and the samples were placed on a hotplate for three
174 hours at 80 °C [35]. Following the acid digest, the supernatant liquor was decanted, and the samples
175 rinsed 3 times with deionised water before being taken to dryness. This process removes calcium
176 and magnesium carbonates (aragonite, calcite, and dolomite), along with other water- or acid-
177 soluble minerals, whilst minimising loss of labile organic matter. Decarbonated samples were
178 analysed on the Elementar instrument. Sample mass was recorded before and after decarbonation,
179 with TOC values corrected to original sample mass.

180

181 Quantifying sediment deposition and erosion

182 Multiple Digital Terrain Models (DTM) at 50 cm horizontal resolution were obtained for the site,
183 derived from airborne LiDAR data [36]. The final pre-breach imagery, from 10 July 2014, pre-dates
184 significant earth movement on site and is therefore unsuitable for use as a baseline. Instead, we
185 have used the first post-breach imagery, from 31 October 2014 (57 days post breach), as a baseline
186 for sediment accumulation on site. Between the date of the breach (4 September 2014) and the date
187 of the imagery used, approximately 37 tides overtopped the creek banks and flooded some of the
188 marsh surface (tides greater than 5.7 m ODN at the nearest available tide gauge, Hinkley Point (data
189 from UK National Tide Gauge Network)). We obtained LiDAR DTMs for eleven further time points
190 after breaching (see Table 1). Downloaded DTMs were processed in Rv4.02 [37] using the “raster”
191 package [38]. Tiles were merged before being clipped by the site area. The site area was defined by
192 manually drawing a polygon around the crest of the flood embankment to remove areas outside of
193 the site. We then restricted analyses to locations subject to tidal inundation which were taken to be
194 those areas below 7.07 m ODN, which is the level of the highest astronomical tides at the nearest
195 port, Burnham-on-Sea [32]. The first DTM available after the breach (31 October 2014) was clipped
196 to locations below 7.07 m and the resulting polygon (with an area of 244.7 ha) used to clip the
197 remaining DTMs.

198 Filtered DTM data should represent the ground elevations, but filtering does not completely remove
199 dense, relatively short vegetation. Vegetation cover at the site in the first three years was sparse
200 (Fig. S1, H Mossman pers. obs.) and so we do not consider this an issue for those years; in the latest
201 year, vegetation cover was denser and extensive, but unvegetated areas remained (H Mossman
202 pers. obs.). The 50 cm resolution cannot account for surface morphology smaller than this (e.g.
203 surface desiccation cracking, which was observed during summer months). We also observed
204 sediment dewatering and shrinkage during dry periods, but these changes were small compared to
205 interannual changes in elevation (Table 1). Pontee and Serato [31] quantified the variation in
206 elevation of control points between years (the same LiDAR datasets we use) and found a mean
207 vertical error of ± 0.04 m.

208 Changes in elevation were calculated between each time point by subtracting the DTM of the first
209 time point from the DTM of the more recent time point. Cumulative changes in elevation were
210 calculated relative to the first post-breach DTM (31 October 2014, 57 days after breach). We
211 calculated the mean elevation change across raster pixels, which was then converted to total change
212 in sediment volume by multiplying by the area covered by the raster DTM. As an alternative way of
213 visualising elevation change in the site, cumulative trajectories of elevation change were calculated
214 for a random subset of 10,000 pixels.

215 To validate the elevation change obtained from LiDAR, we also conducted field measurements of
216 elevation change. We measured elevation change *in situ* at one location within each area (Site A-D
217 and NAT) using 1.5 m metal stakes buried to a depth of 1 m, from which a 50 cm horizontal bar with
218 10 pins was placed and the distance from the tip of the pin to the bar was measured. Stakes were
219 installed on 14 and 15 December 2014, 14 weeks after the breach, and removed at the end of the
220 study 5-7 March 2017 (Table S1). We found good agreement between LiDAR and ground-based
221 measurements of sedimentation rates (Fig. S2).

222

223 Data analysis: variation in sediment carbon

224 Variation in sediment carbon composition was assessed as a function of depth using locally weighted
225 polynomial regression (loess function in R), fitted separately for above and below the agricultural
226 soil-new sediment horizon. We assessed whether there was a difference in the percentage carbon in
227 the newly accreted sediment, natural sediment (pooling locations, time points and depths for both)
228 and the pre-restoration soils from the four land uses using Anova with a Tukey HSD post hoc test.
229 Post-restoration samples from at or below the agricultural horizon were not included in this analysis

230 because (1) we were interested in the carbon accumulating after the restoration in the newly
231 accreted sediment and (2) elevated carbon contents were observed due to the burial of remnant
232 agricultural vegetation as opposed to saltmarsh processes. We calculated the mean and standard
233 deviation of TC in newly accreted sediment, and also calculated the mean and standard deviation of
234 the ratio of TOC and TC. We considered it justified to treat the carbon content of new sediment as
235 coming from a single population (i.e. not varying between years) as (1) the TC of new sediment did
236 not vary with depth in cores and (2) there was no difference in the TC of newly accreted sediment
237 (surface sample of sediment in each year) between years ($F_{1,46} = 0.369$, $P = 0.547$).

238

239 Data analysis: site-level carbon accumulation

240 Site-level carbon accumulation was calculated by (1) multiplying mean change in elevation (m, from
241 DTMs) by site area (m^2) to obtain sediment volume (m^3), (2) multiplying this by bulk density ($t.m^{-3}$) to
242 obtain sediment mass (t), and (3) multiplying this by sediment carbon content (%/100) to obtain
243 total carbon accumulation (t). This was divided by site area to obtain tC/ha. This calculation was
244 repeated with the additional step of multiplying by the ratio to TOC to TC to estimate site level total
245 organic carbon accumulation.

246 As each stage in this calculation involves measurements made with error, we used Monte-Carlo
247 resampling to estimate site-level carbon accumulation while propagating errors from each step. If
248 elevation measurement errors were independent for each DTM pixel in each time point then errors
249 largely cancel out. A more conservative approach is to assume that measurement errors apply
250 systematically to a survey. We do the latter, and take mean elevation change between surveys as
251 coming from a normal distribution with a mean equal to the measured change in elevation, and a
252 standard deviation of 0.04 m based on measurements of control points [31]. Bulk density of newly
253 accreted sediment was sampled from a normal distribution with mean 1.11 and SD 0.27 $t.m^{-3}$.
254 Sediment TC was sampled from a normal distribution with mean 4.37% and SD 0.50%, and the ratio
255 of TOC to TC was sampled from a normal distribution with mean 0.53 and SD 0.08. We took 100,000
256 samples from these distributions to obtain a distribution of carbon accumulation estimates.

257

258 Carbon costs of construction

259 The carbon cost of constructing the wider 400 ha Steart Marshes complex (comprising the 250 ha
260 managed realignment site and neighbouring areas of freshwater wetland) was estimated using the
261 Environment Agency's basic carbon calculator (version 3.1.2, dated 2010 (unpublished); since

262 incorporated within the e:Mission Eric carbon planning tool [39]), with the final estimate produced
263 at the end of construction in January 2015. The calculator included estimated greenhouse gas
264 emissions (in carbon dioxide equivalents, CO₂e) from fuel used for personnel travel, energy use on
265 site within portable accommodation, the emissions embodied in construction materials (considering
266 the weight of material and distance transported to site), and a first order estimate of emissions from
267 machinery fuel usage.

268 As all the materials for the embankment construction were obtained within the footprint of the site,
269 the principal source of emissions was the fuel consumed by construction machinery moving the
270 material within the site. As such, we have refined the estimate of machinery fuel usage based on the
271 known volume of earthworks undertaken for the whole scheme, where fuel consumption was
272 estimated by considering the work required, fuel burn per hour and productivity per hour. Within
273 the managed realignment site, the amount of material that was excavated and transported was
274 calculated by considering the size of the creek network and the volume of the embankment. The
275 material was excavated using an EC250DL Excavator, transported across the site in a Volvo A25D
276 Articulated Dumper Truck (capacity 10.7 m³) and constructed in situ with a D6 Bulldozer and Roller
277 (Table S2). The distance travelled was calculated based on the distance from each section of the
278 embankment to the nearest source of materials, and fuel burn and productivity were obtained from
279 manufacturers and suppliers. Fuel consumption associated with earthworks in other areas of the
280 Steart Marshes complex were based on the volume of earth moved and ground conditions in
281 comparison to the managed realignment site.

282

283

284 **Results**

285 Sedimentation rates

286 The change in elevation measured from DTMs was consistent with field measurements of
287 sedimentation (Fig. S2). Comparison of successive DTMs indicated that the net elevation of the site
288 increased over time (Fig. 2), and by September 2018 714,513 m³ of sediment had accumulated
289 across the site, with an average depth of 0.292 m (Table 1). There was no clear trend in
290 sedimentation rate with time since breach (regression: slope < 0.001, $F_{1,8} = 0.35$, $P = 0.568$),
291 although the most rapid sedimentation was noted immediately following the breach (Table 1). The
292 net elevation of the site increased between most LiDAR surveys. However, in two instances mean
293 elevation decreased between consecutive LiDAR surveys (between June and July 2015, and between
294 March and October 2017), indicating reduction in sediment volume most likely due to dewatering
295 over the summer months.

296 Within the site, elevation change varied from net accretion of 2.2 m to net erosion of 5.0 m (Fig. 2a),
297 with 92% of DTM pixels experiencing net accretion and 7% experiencing net erosion. Some locations
298 experienced considerable erosion (Fig. S3), especially in the main creek which deepened
299 progressively in an upstream direction over time (Fig. S4 see [31] for analysis of the main creek
300 profile). Away from the main creek, most locations increased in elevation. This increase was most
301 evident in the excavated pools at the rear of the site, and to a lesser extent in the side creeks (Fig.
302 2a); 558,648 out of 9,792,179 pixels experienced > 1m of accretion, and 92% of these were located
303 in the two pools.

304

305 Properties of newly accreted sediment

306 The bulk density of newly accreted sediment ranged from 0.553 to 1.568 t m⁻³ (mean = 1.110 ± 0.267
307 SD). There were significant differences in TC between pre-restoration soils of different land uses,
308 newly accreted sediments from within the restoration site and sediments from the existing natural
309 saltmarsh ($F_{5,249}=48.7$, $p<0.001$, Fig. 3). Soils collected prior to restoration from all land uses had
310 significantly lower TC than the newly accreted sediment and the natural saltmarsh sediments, with
311 those from the pre-restoration disturbed (A) and arable (D) areas having the lowest carbon contents
312 (Fig. 3). Sediments from the natural saltmarsh had significantly higher TC ($4.72 \pm 0.58 \%$) than the
313 newly accreting sediment on the restoration site ($4.37 \pm 0.50 \%$). The ratio of TOC to TC was similar
314 in natural saltmarsh and newly accreting sediment on the restoration site (natural = 0.524, restored

315 = 0.529, Fig. 3), giving a TOC of $2.24 \pm 0.33\%$ in newly accreted sediment on the restoration site and
316 $2.44 \pm 0.31\%$ on the natural saltmarsh.

317 There was some spatial variation in the TC of new sediment (significant difference between sampling
318 sites ($F_{3,44} = 5.1$, $P = 0.004$)) but no difference between years ($F_{1,46} = 0.369$, $P = 0.547$). The TC of
319 newly accreted sediment was consistent with depth (Fig. 4). Some samples taken at the horizon with
320 the underlying agricultural soils had very high carbon content, reflecting the terrestrial vegetation
321 buried by the initial inundations of sediment. Below the horizon, TC was lower than in newly
322 accreted sediment and directly comparable to the pre-breach measurements of the agricultural soils
323 (Fig. 4).

324

325 Carbon balance

326 Between 31 October 2014 and 13 September 2018 $714,513 \text{ m}^3$ sediment accumulated on the site.
327 Based on the measured properties of this sediment (mean bulk density of $1.110 \pm 0.267 \text{ t m}^{-3}$ SD, TC
328 of $4.367 \pm 0.499\%$) this equates to $34,642 \text{ tC}$ (95 % confidence intervals = $16,398 - 57,400$)
329 accumulated in sediment, at a rate of $36.6 \text{ tC.ha}^{-1}.\text{yr}^{-1}$ (95% CI = $17.3 - 60.6$). Restricting this to TOC
330 ($53.0 \pm 7.8\%$ of TC) gives $18,343 \text{ tC}$ (95% CI = $8090-32402$) accumulating at $19.4 \text{ tC.ha}^{-1}.\text{yr}^{-1}$ (95% CI =
331 $8.5-34.2$).

332 We estimated the carbon costs of site construction to compare to the carbon accumulation of the
333 site. In total, $489,422 \text{ m}^3$ of material were excavated on site, with $411,397 \text{ m}^3$ used in the
334 construction of the new flood embankments and the remainder used in site landscaping. Moving
335 material across the site resulted in vehicles travelling $69,563 \text{ km}$. Overall, construction of the
336 managed realignment site earthworks required 551,012 litres of diesel fuel to be combusted,
337 resulting in $1,477 \text{ tCO}_2\text{e}$ (403 tC) being emitted (Table S2). An estimated additional 20% of fuel
338 consumption was assumed for the construction of earthworks in other areas of the Steart Marshes
339 complex, giving total emissions associated with machinery fuel usage of $1,772 \text{ tCO}_2\text{e}$ (483 tC).
340 Combining these figures with the estimated emissions from personnel travel, energy use in portable
341 accommodation, and embodied emissions of construction materials from the Environment Agency
342 carbon calculator, gives estimated total construction emissions of $2,762 \text{ tCO}_2\text{e}$ (753 tC). These
343 emissions are equivalent to $\sim 2\%$ of the estimated TC accumulation, or $\sim 4\%$ of the estimated
344 TOC accumulation in the sediments over the 4 year study period, with a carbon payback period on
345 the order of 1 (TC) to 2 (TOC) months.

346

347 **Discussion**

348 We find that Steart Marshes managed realignment has rapidly accumulated carbon since the
349 fronting flood defence embankment was breached, and that this carbon accumulation is two orders
350 of magnitude greater than the carbon costs incurred during site construction. The rate of carbon
351 accumulation at Steart Marshes ($TC = 36.6 \text{ t C.ha}^{-1}.\text{yr}^{-1}$, $TOC = 19.4 \text{ t C.ha}^{-1}.\text{yr}^{-1}$) is considerably higher
352 than has been found at other sites. In the Bay of Fundy, which like the Severn Estuary is hypertidal,
353 carbon accumulation is lower but within the same order of magnitude at $13.29 \text{ t C ha}^{-1} \text{ yr}^{-1}$ [25], but
354 rates at other sites are an order of magnitude lower than at Steart Marshes. For example,
355 saltmarshes in eastern England were reported to accumulate carbon at a rate of $1.04 \text{ t C ha}^{-1} \text{ yr}^{-1}$ for
356 the first 20 years following creation [24], while a recovering saltmarsh in Australia accumulates at a
357 rate of $0.5 \text{ t C ha}^{-1} \text{ yr}^{-1}$ [40].

358 The rate of carbon accumulation in a restored saltmarsh is a product of the rate of sediment
359 accumulation and the carbon content of that sediment, and we can look at both these elements to
360 see if Steart Marshes is unusual. Steart Marshes has experienced rapid sediment accumulation since
361 it was breached (mean rate of increase in elevation = 75 mm yr^{-1} , Table 1). Similarly high accretion
362 rates have been reported from elsewhere in the Severn Estuary system (short-term accretion rates
363 of 60 mm yr^{-1} in young marshes in Bridgwater Bay [41]; around 60 mm yr^{-1} in accreting natural marsh
364 in Portishead [42, 43]) and also in the Bay of Fundy ($>60 \text{ mm yr}^{-1}$ [25]). In comparison, reported
365 sedimentation rates for Tollesbury and Freiston Shore managed realignment sites in eastern England
366 are considerably lower ($< 20 \text{ mm yr}^{-1}$ [44-46]). A recent meta-analysis has indicated that sediment
367 availability is the dominant control on the vertical accretion of coastal wetland restoration projects,
368 with tidal range, elevation within the tidal frame and sea-level rise explaining a smaller amount of
369 observed variation in the vertical accretion rates of saltmarshes [47]. Hypertidal systems such as the
370 Severn Estuary and the Bay of Fundy are characterised by very high energies and dynamic intertidal
371 sedimentation, where the high suspended sediment load (due to the turbulence created by tidal
372 currents and bores) allows deposition during both flood and ebb tides [48]. While the suspended
373 sediment concentrations within the Severn Estuary vary significantly (depending on geographical
374 location, position in the water column, and state of tide), there is a turbidity maxima located in the
375 lower estuary in the vicinity of Bridgwater Bay and the Parrett Estuary (and thus Steart Marshes),
376 with high suspended sediment concentrations typically in the range of 1,000-10,000's mg/l with
377 values often exceeding 100,000 mg/l [49-52]. Much lower suspended sediment concentrations (~ 50 -
378 150 mg/l), and thus lower sediment supply, are reported for the Blackwater Estuary (Tollesbury) and
379 The Wash (Freiston Shore) [53, 54].

380 Sediment carbon content at Steart Marshes is higher than in some managed realignment sites, but is
381 close to the range of values reported elsewhere. Comparison with values from other managed
382 realignments indicates bulk density varies from $0.74 - 1.4 \text{ t m}^{-3}$ [24, 55-57] (cf 1.1 in this study) and
383 carbon content varies from 1.8-4.23% (cf TC 4.4% and TOC 2.2% in this study). Combining all
384 combinations of sediment carbon content and accretion rates gives the space of potential carbon
385 accumulation rates in saltmarsh restored by managed realignment (Fig. 5). This indicates that Steart
386 Marshes has high rates of carbon accumulation because it experiences both high rates of accretion
387 and has relatively high sediment carbon content; thus while neither variable is exceptionally high
388 compared with other values reported in the literature, this combination leads to the exceptionally
389 high rates of carbon accumulation. Lower values of either one of these limits carbon accumulation.
390 For example, In natural saltmarshes in China, carbon accumulation rates are low ($0.35-3.61 \text{ tC ha}^{-1} \text{ yr}^{-1}$)
391 despite accretion of 20 mm yr^{-1} because of low sediment carbon densities ($< 0.01 \text{ g cm}^{-3}$) [58].

392 This variability in carbon accumulation rates between sites highlights the need for further work to
393 support large-scale assessments of the carbon sequestration potential of saltmarsh restoration. For
394 example, TOC accumulation rates at Steart Marshes are over 18 times higher (and TC accumulation
395 rates are over 35 times higher) than those used in a recent study to estimate the UK's carbon
396 sequestration potential [59], while Mossman et al. [28] found ~13 fold variation in the potential
397 amount of carbon accumulated by restored saltmarshes in the UK based on published estimates of
398 carbon accumulation.

399 If the high rate of carbon accumulation at Steart Marshes is unusual, is the conclusion that
400 saltmarshes restored by managed realignment rapidly pay off their carbon construction costs
401 applicable to other sites? We can evaluate this by mapping our estimates of construction carbon
402 costs onto the potential carbon accumulation space (Fig. 5). Most combinations of accretion rate
403 and sediment carbon content would pay off construction costs of a 250 ha site within a year, and
404 even a site with low carbon accumulation rates (Tollesbury managed realignment, eastern England)
405 would be close to breaking even with its carbon construction costs over one year.

406 Our analysis assumes that soil properties (soil carbon, bulk density) come from a single statistical
407 population across the site and over time. However, there were small differences in the carbon
408 content of new sediment across the site. The reasons for this are unclear, but could relate to spatial
409 variation in algal films and vegetation establishment across the site. If the drivers of variation in
410 sediment carbon across the site were known this could be used to scale-up and refine estimates, but
411 this is not currently possible. The bulk density of sediment would be expected to exhibit temporal
412 variation, with lower bulk density (but greater sediment volume) when sediment is waterlogged (e.g.

413 winter, spring), and higher bulk density (but lower sediment volume) when sediment is dry (e.g.
414 summer, early autumn). Our bulk density measurements come from spring and summer, so should
415 capture this temporal variation in bulk density. However, explicitly quantifying temporal variation in
416 bulk density would allow temporal coupling with sediment accumulation data and thus refined
417 quantification of intra-annual variation in carbon accumulation – apparent reductions in carbon
418 stocks over the summer when sediment volume reduced may not occur in reality because of a
419 concurrent increase in sediment bulk density.

420

421 Future changes in carbon accumulation

422 Although we found the fastest rates of accretion shortly following breaching, we did not find a
423 statistically significant reduction in accretion rates. However, a reduction in accretion rates would be
424 expected as the saltmarsh develops. This is because accretion rates tend to be faster at lower
425 elevations which experience more frequent tidal inundation [60], and as these lower areas increase
426 in elevation they experience fewer inundations, and thus slower accretion. Indeed, space-for-time
427 substitutions indicate that carbon accumulation rates slow over time [24]. It is likely that carbon
428 accumulation rates at Steart Marshes would slow with longer monitoring. Assuming there is
429 sufficient sediment available (as very likely in this case), accretion at managed realignments is
430 expected to occur until the site is a level plane accreting in line with sea-level rise [60]. Natural
431 saltmarsh surrounding the site occurs at elevations of 6.5 m, where if accretion at Steart Marshes
432 stabilised at this level this would result in a TC accumulation in excess of 100 ktC (TOC in excess of 50
433 ktC), of which 33% has currently been accumulated. Even after this point, saltmarshes can continue
434 to accrete with sea-level rise assuming there is sufficient sediment [61], which at 3.7mm yr⁻¹ [62]
435 would result in continued TC accumulation of 439 t C yr⁻¹ and TOC accumulation of 225 t C yr⁻¹ at
436 Steart Marshes assuming no change in sediment carbon content.

437

438 Challenges with determining the carbon budget of a managed realignment

439 Our results indicate that carbon accumulation at Steart Marshes greatly exceeds construction costs.
440 However, there are a number of uncertainties that, while highly likely not to affect this qualitative
441 conclusion, would need to be considered to refine the quantitative carbon budget (Table 2, [28]).
442 Some assumptions, such as assuming the carbon content of sediment lost is the same as sediment
443 gained, are likely to mean our estimate of carbon accumulation is conservative (Table 2). Others,

444 such as not accounting for greenhouse gas emissions following site flooding, will offset some of the
445 carbon accumulation benefit of the site (Table 2).

446 A particularly challenging element of quantifying the carbon budget of a restored saltmarsh is
447 determining the nature and origin of the carbon accumulated in sediment. This is critical to establish
448 the additionality test needed for carbon credits and offsetting credits (e.g. Verified Carbon Standard
449 Methodology VM0033 [63]), where in simple terms, carbon credits should only be generated
450 through the creation of new net sinks of atmospheric carbon. In the coastal and marine
451 environment, this requires consideration of the relative importance of allochthonous and
452 autochthonous carbon, downstream effects, and both organic carbon and biogenic carbonate
453 inputs. For example, concerns regarding additionality have led to variable treatment of allochthonous
454 carbon, where creating a new apparent store may be depleting supply to an adjacent system (i.e. the
455 carbon would have been stored elsewhere in the absence of the project). Tools such as biomarkers
456 [64] and stable isotopes are being developed to better identify sources of carbon [18], where
457 integrated studies of interconnected blue carbon ecosystems across the land-ocean transect would
458 help address the appropriateness of accounting for allochthonous carbon. While lithogenic
459 carbonates should clearly be excluded from estimates of carbon storage (as they comprise fossil C
460 that has not been in recent contact with the atmosphere), the treatment of biogenic carbonates is
461 more complex. Carbonate production is a source of CO₂ to the atmosphere, while carbonate
462 dissolution is a sink [65], where the relative balance of these processes and the impact on ecosystem
463 carbon budgets (which also depends on whether the carbonate is imported or produced in-situ, and
464 the role of carbonates in stabilising organic carbon stores) remains a significant uncertainty in blue
465 carbon science [18].

466 **Conclusions**

467 Our results show that at Steart Marshes fast rates of sediment accumulation and high sediment
468 carbon content combine to result in exceptionally fast carbon accumulation rates. Carbon
469 accumulation at Steart Marshes over the first four years following reinstatement of tidal flow is two
470 orders of magnitude larger than the carbon costs of site construction. Thus qualitatively, it is clear
471 that the creation of the site by managed realignment has delivered benefits for carbon storage and
472 sequestration, and other sites with lower carbon accumulation rates are likely to rapidly pay off their
473 construction carbon debt. However, there are numerous uncertainties that would need to be
474 resolved in order to move to a fully quantitative carbon budget for restored saltmarshes.

475

476 **Acknowledgements**

477 We thank the Wildfowl and Wetlands Trust, particularly Alys Laver and Tim McGrath, for access to
478 the site and their ongoing enthusiasm and support. We thank Grace Biddle, Colin Hill and David
479 McKendry for their work in the laboratory. This study uses data from UK National Tide Gauge
480 Network, owned and operated by the Environment Agency, and provided by the British
481 Oceanographic Data Centre.

482

483 **References**

- 484 1. Friedlingstein P, O'Sullivan M, Jones MW, Andrew RM, Hauck J, Olsen A, et al. Global Carbon
485 Budget 2020. *Earth Syst Sci Data*. 2020;12(4):3269-340. doi: 10.5194/essd-12-3269-2020.
- 486 2. Guo LB, Gifford RM. Soil carbon stocks and land use change: a meta analysis. *Global Change
487 Biology*. 2002;8(4):345-60. doi: <https://doi.org/10.1046/j.1354-1013.2002.00486.x>.
- 488 3. Sullivan MJP, Lewis SL, Affum-Baffoe K, Castilho C, Costa F, Sanchez AC, et al. Long-term
489 thermal sensitivity of Earth's tropical forests. *Science*. 2020;368(6493):869-74.
- 490 4. McLeod E, Chmura GL, Bouillon S, Salm R, Björk M, Duarte CM, et al. A blueprint for blue
491 carbon: toward an improved understanding of the role of vegetated coastal habitats in sequestering
492 CO₂. *Frontiers in Ecology and the Environment*. 2011;9(10):552-60. doi:
493 <https://doi.org/10.1890/110004>.
- 494 5. McOwen CJ, Weatherdon LV, Van Bochove J-W, Sullivan E, Blyth S, Zockler C, et al. A global
495 map of saltmarshes. *Biodiversity data journal*. 2017;(5).
- 496 6. Ouyang X, Lee SY. Updated estimates of carbon accumulation rates in coastal marsh
497 sediments. *Biogeosciences*. 2014;11(18):5057-71.
- 498 7. Barbier EB, Hacker SD, Kennedy C, Koch EW, Stier AC, Silliman BR. The value of estuarine and
499 coastal ecosystem services. *Ecological Monographs*. 2011;81(2):169-93. doi: 10.1890/10-1510.1.
500 PubMed PMID: WOS:000290707600001.
- 501 8. Murray NJ, Clemens RS, Phinn SR, Possingham HP, Fuller RA. Tracking the rapid loss of tidal
502 wetlands in the Yellow Sea. *Frontiers in Ecology and the Environment*. 2014;12(5):267-72. doi:
503 10.1890/130260.
- 504 9. Duarte CM, Dennison WC, Orth RJW, Carruthers TJB. The charisma of coastal ecosystems:
505 addressing the imbalance. *Estuaries and coasts*. 2008;31(2):233-8.
- 506 10. Bull JW, Milner-Gulland EJ. Choosing prevention or cure when mitigating biodiversity loss:
507 Trade-offs under 'no net loss' policies. *Journal of Applied Ecology*. 2020;57(2):354-66.
- 508 11. Li S, Xie T, Pennings SC, Wang Y, Craft C, Hu M. A comparison of coastal habitat restoration
509 projects in China and the United States. *Scientific Reports*. 2019;9(1):14388. doi: 10.1038/s41598-
510 019-50930-6.
- 511 12. Stewart-Sinclair PJ, Purandare J, Bayraktarov E, Waltham N, Reeves S, Statton J, et al. Blue
512 Restoration – Building Confidence and Overcoming Barriers. *Frontiers in Marine Science*. 2020;7:748.
- 513 13. Salzman J, Bennett G, Carroll N, Goldstein A, Jenkins M. The global status and trends of
514 Payments for Ecosystem Services. *Nature Sustainability*. 2018;1(3):136-44.
- 515 14. Vieira da Silva L, Everard M, Shore RG. Ecosystem services assessment at Steart Peninsula,
516 Somerset, UK. *Ecosystem Services*. 2014;10:19-34. doi:
517 <https://doi.org/10.1016/j.ecoser.2014.07.008>.
- 518 15. Serrano O, Lovelock CE, B. Atwood T, Macreadie PI, Canto R, Phinn S, et al. Australian
519 vegetated coastal ecosystems as global hotspots for climate change mitigation. *Nature
520 Communications*. 2019;10(1):4313. doi: 10.1038/s41467-019-12176-8.

521 16. Needelman BA, Emmer IM, Emmett-Mattox S, Crooks S, Megonigal JP, Myers D, et al. The
522 Science and Policy of the Verified Carbon Standard Methodology for Tidal Wetland and Seagrass
523 Restoration. *Estuaries and Coasts*. 2018;41(8):2159-71. doi: 10.1007/s12237-018-0429-0.

524 17. Wedding LM, Moritsch M, Verutes G, Arkema K, Hartge E, Reiblich J, et al. Incorporating blue
525 carbon sequestration benefits into sub-national climate policies. *Global Environmental Change*.
526 2021;102206. doi: <https://doi.org/10.1016/j.gloenvcha.2020.102206>.

527 18. Macreadie PI, Anton A, Raven JA, Beaumont N, Connolly RM, Friess DA, et al. The future of
528 Blue Carbon science. *Nature Communications*. 2019;10(1):3998. doi: 10.1038/s41467-019-11693-w.

529 19. Lawrence PJ, Smith GR, Sullivan MJ, Mossman HL. Restored saltmarshes lack the topographic
530 diversity found in natural habitat. *Ecological engineering*. 2018;115:58-66.

531 20. Mossman HL, Davy AJ, Grant A. Does managed coastal realignment create saltmarshes with
532 'equivalent biological characteristics' to natural reference sites? *Journal of Applied Ecology*.
533 2012;49(6):1446-56. doi: 10.1111/j.1365-2664.2012.02198.x.

534 21. Moreno-Mateos D, Power ME, Comín FA, Yockteng R. Structural and Functional Loss in
535 Restored Wetland Ecosystems. *PLOS Biology*. 2012;10(1):e1001247. doi:
536 10.1371/journal.pbio.1001247.

537 22. Moritsch MM, Young M, Carnell P, Macreadie PI, Lovelock C, Nicholson E, et al. Estimating
538 blue carbon sequestration under coastal management scenarios. *Science of The Total Environment*.
539 2021;777:145962. doi: <https://doi.org/10.1016/j.scitotenv.2021.145962>.

540 23. MacDonald MA, de Ruyck C, Field RH, Bedford A, Bradbury RB. Benefits of coastal managed
541 realignment for society: Evidence from ecosystem service assessments in two UK regions. *Estuarine,
542 Coastal and Shelf Science*. 2020;244:105609. doi: <https://doi.org/10.1016/j.ecss.2017.09.007>.

543 24. Burden A, Garbutt A, Evans CD. Effect of restoration on saltmarsh carbon accumulation in
544 Eastern England. *Biology Letters*. 2019;15(1):20180773.

545 25. Wollenberg JT, Ollerhead J, Chmura GL. Rapid carbon accumulation following managed
546 realignment on the Bay of Fundy. *PLOS ONE*. 2018;13(3):e0193930. doi:
547 10.1371/journal.pone.0193930.

548 26. Hoogsteen MJJ, Lantinga EA, Bakker EJ, Groot JCJ, Tittonell PA. Estimating soil organic carbon
549 through loss on ignition: effects of ignition conditions and structural water loss. *European Journal of
550 Soil Science*. 2015;66(2):320-8. doi: <https://doi.org/10.1111/ejss.12224>.

551 27. The Greenhouse Gas Protocol. The GHG Protocol for Project Accounting. World Business
552 Council for Sustainable Development and World Resources Institute; 2005.

553 28. Mossman HL, Sullivan MJP, Dunk RM, Rae S, Sparkes RT, Pontee, N. Created coastal wetlands
554 as carbon stores: potential challenges and opportunities. In: Humphreys J, Little S, editors.
555 Challenges in Estuarine and Coastal Science: Estuarine and Coastal Sciences Association 50th
556 Anniversary Volume. UK: Pelagic Publishing; 2021.

557 29. Scott J, Pontee N, McGrath T, Cox R, Philips M. Delivering Large Habitat Restoration
558 Schemes: Lessons from the Steart Coastal Management Project. *Coastal Management: Changing
559 coast, changing climate, changing minds*: ICE Publishing; 2016. p. 663-74.

560 30. British Geological Society. Geology of Britain [cited 2021 21 April]. Available from:
561 <https://mapapps.bgs.ac.uk/geologyofbritain/home.html>.

562 31. Pontee N, Serato B. Nearfield erosion at the steart marshes (UK) managed realignment
563 scheme following opening. *Ocean & Coastal Management*. 2019;172:64-81.

564 32. UK Hydrographic Office. Admiralty Tide Tables Volume 1: United Kingdom and Ireland
565 (Including European Channel Ports). Taunton, UK: The United Kingdom Hydrographic Office; 2010.

566 33. Pontee NI. Impact of managed realignment design on estuarine water levels. *Proceedings of
567 the Institution of Civil Engineers - Maritime Engineering*. 2015;168(2):48-61.

568 34. Rowell DL. Soil science: Methods & applications: Routledge; 2014.

569 35. Sparkes RB, Lin I-T, Hovius N, Galy A, Liu JT, Xu X, et al. Redistribution of multi-phase
570 particulate organic carbon in a marine shelf and canyon system during an exceptional river flood:

571 Effects of Typhoon Morakot on the Gaoping River–Canyon system. *Marine Geology*. 2015;363:191-
572 201. doi: <https://doi.org/10.1016/j.margeo.2015.02.013>.

573 36. Defra. LiDAR Composite DTM - 0.5 m. Open Government Licence v3.0
<https://environment.data.gov.uk/DefraDataDownload/?Mode=survey2020> [25 January 2021].

574 37. R Development Core Team. R: A language and environment for statistical computing. 3.5.0
575 ed. Vienna: R Foundation for Statistical Computing; 2018.

576 38. Hijmans RJ. raster: Geographic Data Analysis and Modeling. R package version 3.3-6. 2020.

577 39. Environment Agency. Eric carbon planning tool training package:
https://www.ericenvironmentagency.co.uk/story_html5.html?lms=1 [cited 2021 08/10/2021].

578 40. Gulliver A, Carnell PE, Trevathan-Tackett SM, Duarte de Paula Costa M, Masqué P,
579 Macreadie PI. Estimating the Potential Blue Carbon Gains From Tidal Marsh Rehabilitation: A Case
580 Study From South Eastern Australia. *Frontiers in Marine Science*. 2020;7:403.

581 41. Ranwell DS. Spartina salt marshes in southern England: II. Rate and seasonal pattern of
582 sediment accretion. *The Journal of Ecology*. 1964;79-94.

583 42. Allen JRL, Duffy MJ. Medium-term sedimentation on high intertidal mudflats and salt
584 marshes in the Severn Estuary, SW Britain: the role of wind and tide. *Marine Geology*. 1998;150(1-
585 4):1-27.

586 43. Allen JRL, Duffy MJ. Temporal and spatial depositional patterns in the Severn Estuary,
587 southwestern Britain: intertidal studies at spring–neap and seasonal scales, 1991–1993. *Marine
588 Geology*. 1998;146(1-4):147-71.

589 44. Brown SL, Pinder A, Scott L, Bass J, Rispin E, Brown S, et al. Wash Banks Flood Defence
590 Scheme Freiston Environmental Monitoring 2002-2006. Report to Environment Agency,
591 Peterborough. Centre for Ecology and Hydrology, Dorset, UK: 2007.

592 45. Garbutt A. Bed level change within the Tollesbury managed realignment site, Blackwater
593 estuary, Essex, UK between 1995 and 2007. NERC Environmental Information Data Centre; 2018.

594 46. Spencer T, Friess DA, Möller I, Brown SL, Garbutt RA, French JR. Surface elevation change in
595 natural and re-created intertidal habitats, eastern England, UK, with particular reference to Freiston
596 Shore. *Wetlands Ecology and Management*. 2012;20(1):9-33. doi: 10.1007/s11273-011-9238-y.

597 47. Liu Z, Fagherazzi S, Cui B. Success of coastal wetlands restoration is driven by sediment
598 availability. *Communications Earth & Environment*. 2021;2(1):1-9.

599 48. Archer AW. World's highest tides: Hypertidal coastal systems in North America, South
600 America and Europe. *Sedimentary Geology*. 2013;284-285:1-25. doi:
601 <https://doi.org/10.1016/j.sedgeo.2012.12.007>.

602 49. Thorn MFC, Burt TN. Sediments and metal pollutants in a turbid tidal estuary. *Canadian
603 Journal of Fisheries and Aquatic Sciences*. 1983;40(S1):s207-s15.

604 50. Mantz PA, Wakeling HL. Aspects of sediment movement near to Bridgwater Bay bar, Bristol
605 Channel. *Proceedings of the Institution of Civil Engineers*. 1982;73(1):1-23.

606 51. Derbyshire EJ, West JR. Turbulence and cohesive sediment transport in the Parrett estuary.
607 Turbulence: Perspectives on Flow and Sediment Transport Wiley, Chichester. 1993:215-47.

608 52. Manning AJ, Langston WJ, Jonas PJC. A review of sediment dynamics in the Severn Estuary:
609 Influence of flocculation. *Marine Pollution Bulletin*. 2010;61(1):37-51. doi:
610 <https://doi.org/10.1016/j.marpolbul.2009.12.012>.

611 53. French JR. Numerical simulation of vertical marsh growth and adjustment to accelerated
612 sea-level rise, North Norfolk, U.K. *Earth Surface Processes and Landforms*. 1993;18(1):63-81. doi:
613 <https://doi.org/10.1002/esp.3290180105>.

614 54. Spearman J. The development of a tool for examining the morphological evolution of
615 managed realignment sites. *Continental Shelf Research*. 2011;31(10):S199-S210.

616 55. Clapp J. Managed realignment in the Humber estuary: factors influencing sedimentation.
617 2009. Unpublished PhD thesis, University of Hull.

620 56. Spencer KL, Carr SJ, Diggens LM, Tempest JA, Morris MA, Harvey GL. The impact of pre-
621 restoration land-use and disturbance on sediment structure, hydrology and the sediment
622 geochemical environment in restored saltmarshes. *Science of the Total Environment*. 2017;587:47-58.

623 57. Blackwell MSA, Yamulki S, Bol R. Nitrous oxide production and denitrification rates in
624 estuarine intertidal saltmarsh and managed realignment zones. *Estuarine, Coastal and Shelf Science*.
625 2010;87(4):591-600.

626 58. Chen J, Wang D, Li Y, Yu Z, Chen S, Hou X, et al. The carbon stock and sequestration rate in
627 tidal flats from coastal China. *Global Biogeochemical Cycles*. 2020;34(11):e2020GB006772.

628 59. Bradfer-Lawrence T, Finch T, Bradbury RB, Buchanan GM, Midgley A, Field RH. The potential
629 contribution of terrestrial nature-based solutions to a national 'net zero' climate target. *Journal of
630 Applied Ecology*. 2021;n/a(n/a). doi: <https://doi.org/10.1111/1365-2664.14003>.

631 60. Pontee N. Accounting for siltation in the design of intertidal creation schemes. *Ocean &
632 coastal management*. 2014;88:8-12.

633 61. Schuerch M, Spencer T, Temmerman S, Kirwan ML, Wolff C, Lincke D, et al. Future response
634 of global coastal wetlands to sea-level rise. *Nature*. 2018;561(7722):231-4. doi: [10.1038/s41586-018-0476-5](https://doi.org/10.1038/s41586-018-0476-5).

635 62. Met Office. UKCP09: Gridded observation data sets. 2009.

636 63. Emmer I, Needelman B, Emmett-Mattox S, Crooks S, Megonigal P, Myers D, et al. VM0033
637 Methodology for tidal wetland and seagrass restoration. Version 1.0. Verra. Verified Carbon
638 Standard, 2015.

639 64. Bischoff J, Sparkes RB, Doğrul Selver A, Spencer RGM, Gustafsson Ö, Semiletov IP, et al.
640 Source, transport and fate of soil organic matter inferred from microbial biomarker lipids on the East
641 Siberian Arctic Shelf. *Biogeosciences*. 2016;13(17):4899-914.

642 65. Saderne V, Geraldi NR, Macreadie PI, Maher DT, Middelburg JJ, Serrano O, et al. Role of
643 carbonate burial in Blue Carbon budgets. *Nature communications*. 2019;10(1):1-9.

644 66. Centre for Ecology and Hydrology. Land Cover Map 2007 [SHAPE geospatial data], Scale
645 1:250000. Updated: 18 July 2008.: EDINA Environment Digimap Service,
646 <<https://digimap.edina.ac.uk>>; 2007.

647 67. Environment Agency. Steart Coastal Management Project Environmental Statement: Report
648 produced by Halcrow for the Environment Agency. Bristol, UK: Environment Agency; 2011. p. 178pp

649 68. Getmapping. High Resolution (25cm) Vertical Aerial Imagery [JPG geospatial data], Scale
650 1:500, Updated: 25 October 2014. EDINA Aerial Digimap Service, <https://digimap.edina.ac.uk>; 2014.

651 69. Burden A, Garbutt RA, Evans CD, Jones DL, Cooper DM. Carbon sequestration and
652 biogeochemical cycling in a saltmarsh subject to coastal managed realignment. *Estuarine, Coastal
653 and Shelf Science*. 2013;120:12-20.

654 70. Jacobs. Final Far Field Effect & Channel Exit: Review and summary – Note 6. Report prepared
655 for the Environment Agency by Jacobs. 2019. p. 39pp.

656 71. Adams CA, Andrews JE, Jickells T. Nitrous oxide and methane fluxes vs. carbon, nitrogen and
657 phosphorous burial in new intertidal and saltmarsh sediments. *Science of the Total Environment*.
658 2012;434:240-51.

660

661

662 **Supporting information**

663 **Table S1.** Field sampling dates and information. Samples highlighted in bold are those selected for
664 the quantification of total organic carbon. Access issues prevented sampling at some locations in
665 March 2015 and September 2016. We assessed the consequence of the additional uneven sampling
666 by removing samples from these two time periods and recalculating the mean carbon content in
667 newly accreted sediment. The value differed by less than 1% of the original value (i.e. 4.367% vs
668 4.372%), so we retain all samples in the data presented in the manuscript.

669 **Table S2.** Summary of the fuel consumption and t.CO₂ emitted by construction vehicles in the
670 construction of Steart Marshes.

671 **Figure S1.** Photographs of sampling areas (Sites A-D).

672 **Figure S2.** Relationship between elevation change measured with LiDAR derived-DTMs and in situ
673 measurements with pins. In situ measured data (x axis) show difference in elevation between
674 December 2014 (3 months after restoration) and March 2017. Left: Compares in situ data to
675 elevation changes derived from LiDAR data taken in October 2014 and March 2017, and Right
676 compares elevation changes between January 2015 and March 2017. No LiDAR images are available
677 for December 2014. Solid lines show a 1:1 relationship and the dashed lines show the actual
678 relationship (linear regression) between DTM-derived and in situ measurements (dash lines Left: $R^2 =$
679 0.775, $P < 0.001$; Right $R^2 = 0.686$, $P = 0.002$). LiDAR measurements are strongly related to in situ
680 measurements and are not systematically biased when sampling periods are more closely matched
681 (i.e. Right).

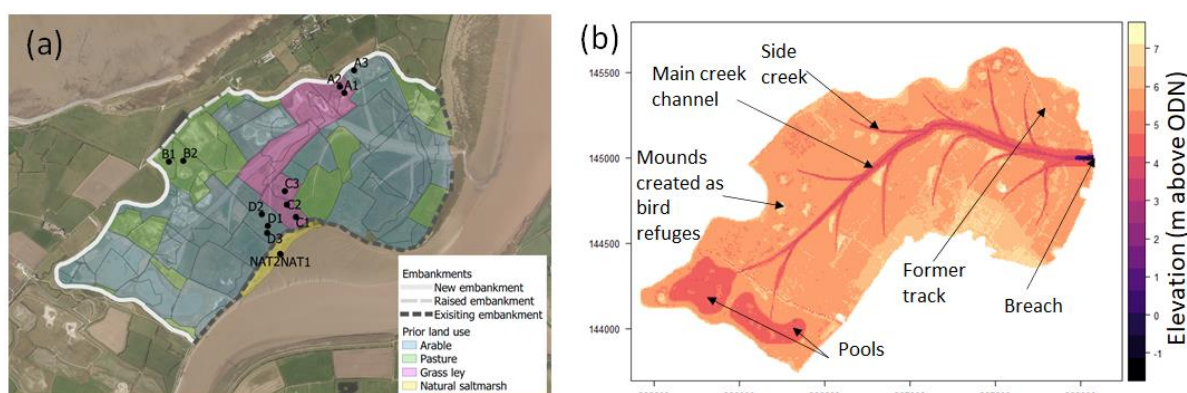
682

683 **Figure S3.** Cumulative elevation change trajectories of a sample of 1000 DTM pixels.

684

685 **Figure S4.** Cumulative change in elevation for each LiDAR survey.

686

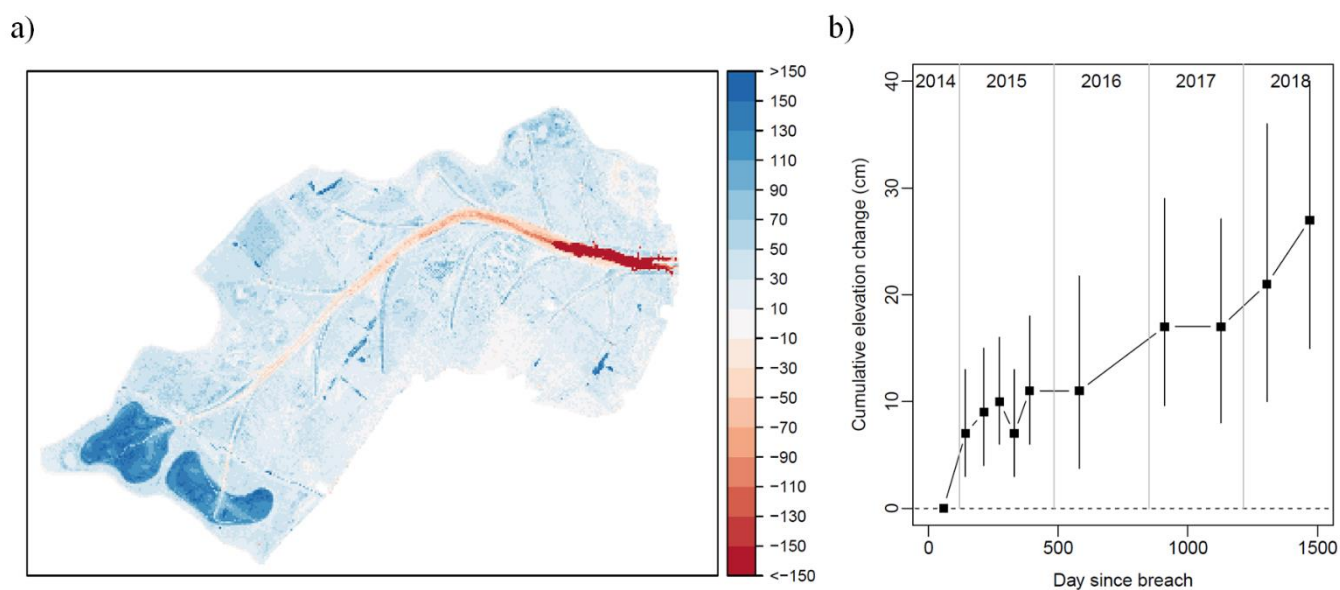


687

688 **Figure 1.** Design and construction elements of Steart managed realignment, Somerset, UK. a) Land
689 use prior to the start of site construction in 2012, and locations of sampling points and the flood
690 embankments constructed (new) or modified (raised) during the project; existing embankments that
691 remained after the project are also shown. Land use was derived from Centre for Ecology and
692 Hydrology Land Cover Map 2007 [66] and the project environmental statement [67]. Base aerial
693 image from 2014 [68]. b) Elevations across the site showing design and location of creek network,
694 lagoons and islands. The location of the breach is also shown. Elevations based on LiDAR data from
695 October 2014 [36].

696

697

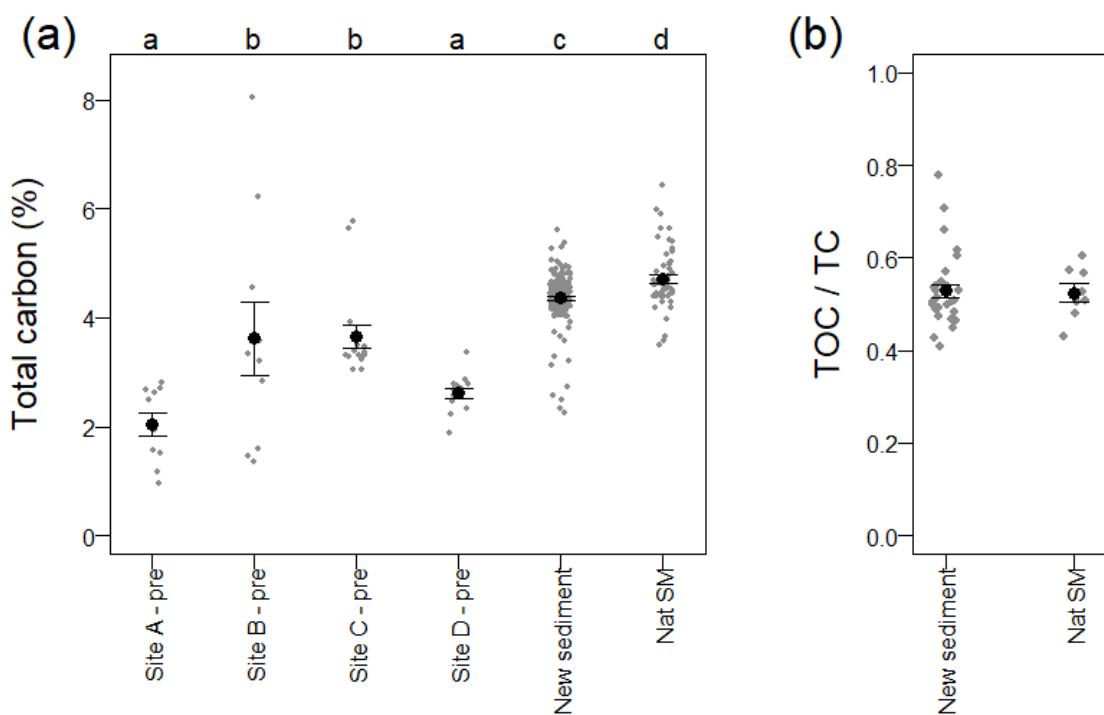


698

699 **Figure 2.** Cumulative sedimentation at Steart Marshes calculated from Lidar DTMs. (a) Change in
700 elevation (cm) between 13/09/2018 (1470 days since breach) and 31/10/2014 (57 days since
701 breach). (b) Cumulative change in elevation over time for individual 50x50 cm pixels. Points show
702 median cumulative change for a random sample of 10,000 pixels. Error bars show the interquartile
703 range for the same sample of pixels.

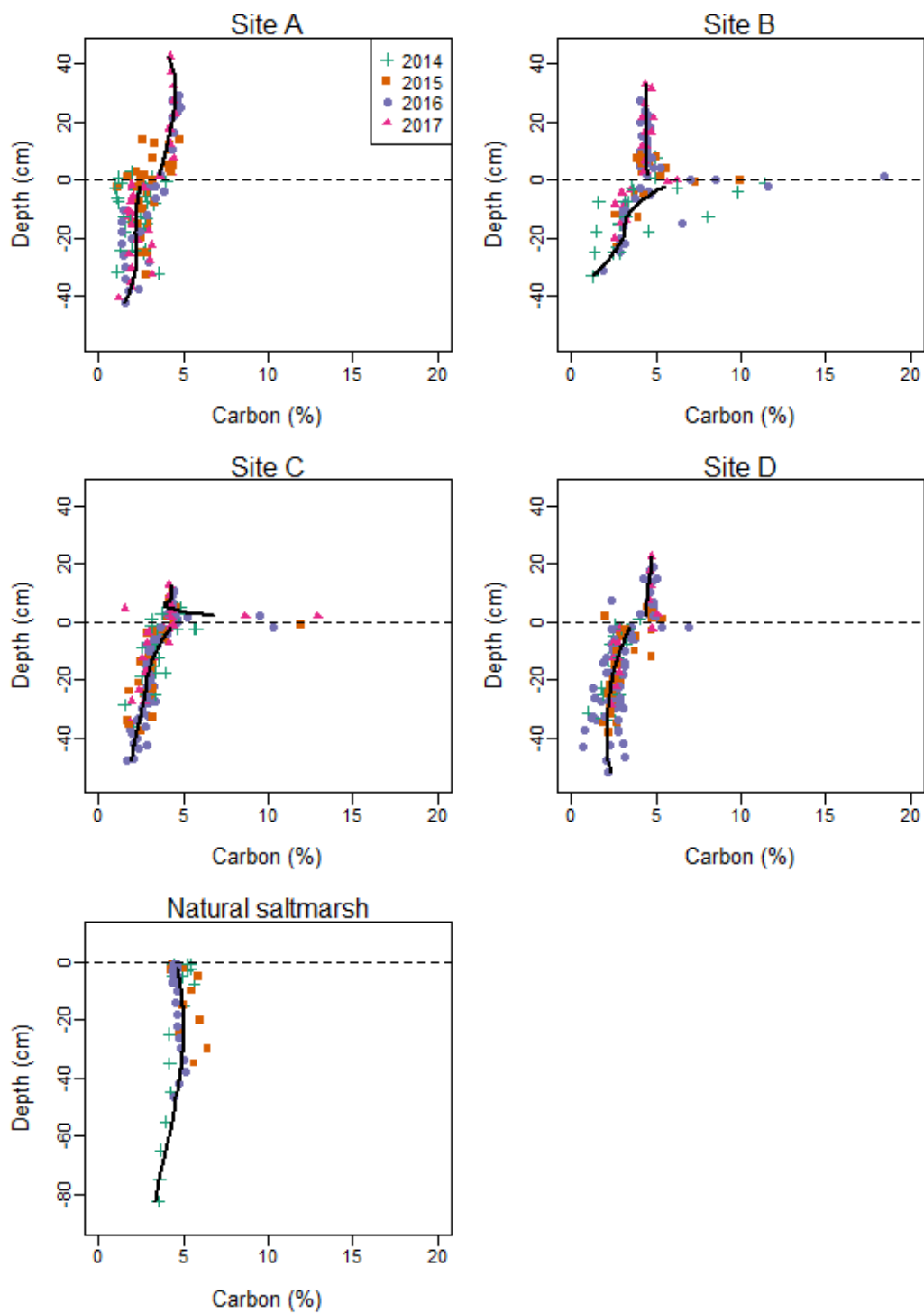
704

705



706

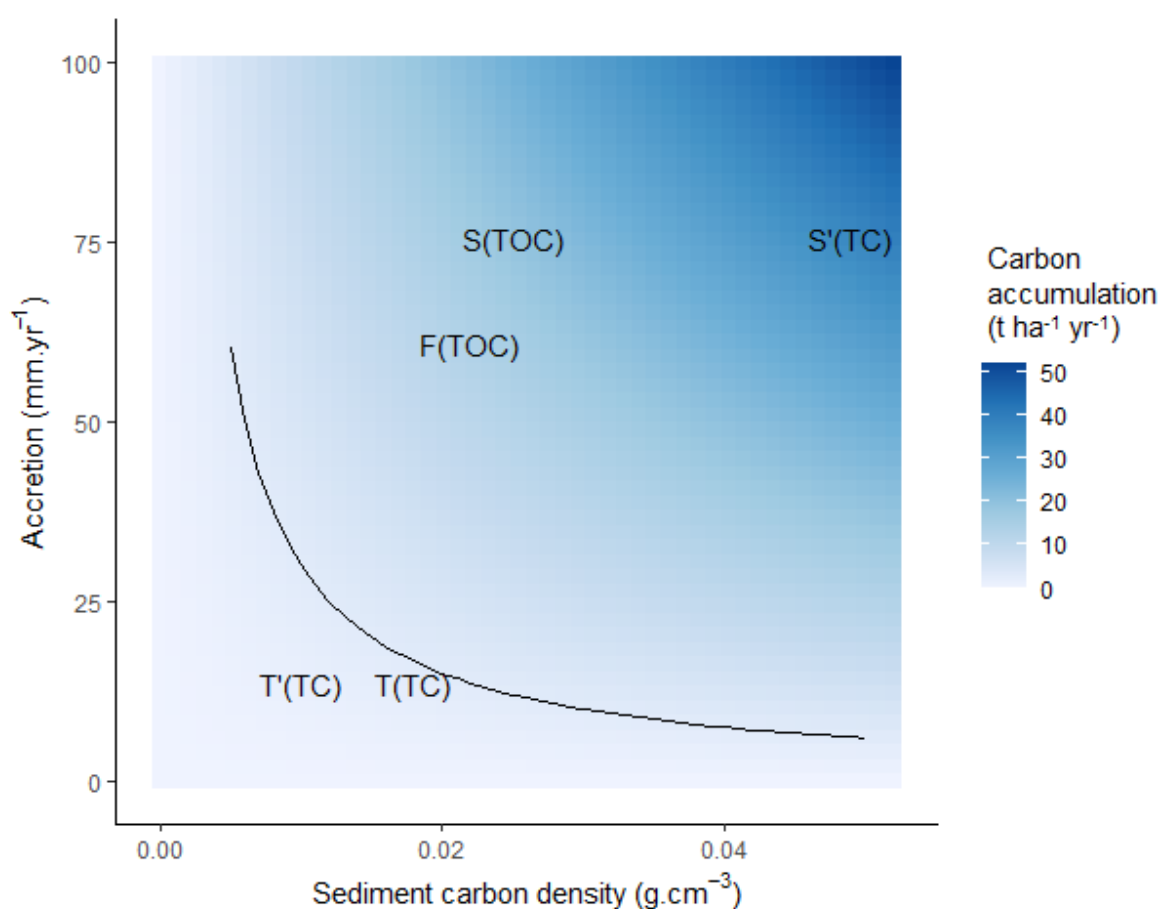
707 **Figure 3.** Proportion of total carbon in soil and sediment samples collected from Steart Marshes
708 before and after the restoration of tidal inundation. Soil samples were collected prior to restoration
709 from an area heavily disturbed during construction (site A), an area of pasture (site B), grass ley (site
710 C) and arable (site D). 'New sediment' are samples of newly accumulated sediments from the
711 restored site after restoration, with data from all locations and time points pooled. Sediment was
712 also collected from an adjacent natural saltmarsh. Differing letters denote significant differences in
713 the carbon content of sediments between locations ($P < 0.05$).



714

715 **Figure 4.** Relationship between soil carbon content and depth. Cores were taken each year at three
716 locations in each starting land-use. Depths are expressed relative to the horizon between
717 agricultural soil and newly deposited sediment, except for natural saltmarsh where depths are from
718 the surface (note difference in y-axis scale for natural saltmarsh). Lines show fits of locally weighted
719 polynomial (loess) models pooling data across locations and years. Loess models have been fit to
720 new sediment (depth > 2 cm) and old sediment (depth < -2 cm) to reduce the effect of vegetation on
721 the horizon.

722



723

724 **Figure 5.** Carbon accumulation potential ($\text{tC ha}^{-1} \text{yr}^{-1}$) of saltmarsh restored by managed realignment.
725 Values from Steart (S and S', this study) and published studies at Tollesbury (T [high marsh] and T'
726 [low marsh] from [45, 69]) and the Bay of Fundy (F, [25]) are shown. TC indicates total carbon
727 sediment carbon density, and TOC indicates total organic carbon sediment carbon density. The solid
728 line delineates the carbon accumulation rate that would be needed for a site to break even with the
729 per hectare construction carbon costs calculated for Steart in one year. Values to the bottom left of
730 the line fail to break even in a year.

731

732 **Table 1.** Sedimentation at Steart Marshes measured by comparing Lidar DTMs to a baseline survey
733 on 31 October 2014, 57 days after sea defences were breached.

Survey date	Days since breach	Sedimentation rate (m yr ⁻¹)		Mean sediment depth (m)	Cumulative sediment volume (m ³)	Cumulative carbon (95% confidence intervals) (t)	Cumulative organic carbon (95% confidence intervals) (t)
		since start*	since previous survey				
24/01/2015	142	0.449	0.449	0.104	255646	12338 (2620-25697)	6533 (1308-14101)
05/04/2015	213	0.258	0.029	0.110	269282	13050 (3178-26582)	6910 (1617-14704)
04/06/2015	273	0.217	0.112	0.128	314126	15186 (4750-29578)	8041 (2384-16392)
31/07/2015	330	0.127	-0.216	0.095	231555	11271 (1708-24269)	5968 (875-13455)
28/09/2015	389	0.153	0.277	0.139	341190	16491 (5625-31303)	8732 (2837-17431)
07/04/2016	581	0.110	0.034	0.157	384983	18626 (7016-34395)	9863 (3536-19060)
02/03/2017	910	0.092	0.064	0.215	525227	25507 (11315-44184)	13506 (5614-24670)
06/10/2017	1128	0.067	-0.028	0.198	483641	23490 (10045-41212)	12438 (5004-23134)
01/04/2018	1305	0.073	0.105	0.249	608657	29541 (13545-49886)	15642 (6733-28069)
13/09/2018	1470	0.075	0.096	0.292	714513	34642 (16398-57400)	18343 (8090-32402)

734

735 **Table 2.** Elements that require consideration in the quantification of a full carbon budget of a
736 managed realignment site. The aspects included in this study, the approaches to these that we took,
737 and any implications of these approaches are also given.

Element	Approach in this study	Rationale of approach and its implications
Amount of sediment gained and lost within the site	Measured using LiDAR derived DTMs, validated against <i>in situ</i> measurements.	Baseline LiDAR is 57 days after breach and ~37 tides covered at least some of the marsh surface between the breach and this LiDAR image, so some post-breach sedimentation will have been missed. This approach has likely underestimated total carbon gained.
Changes in intertidal habitat in the wider estuary: the realignment site might cause changes to the sediment dynamics of the wider estuary. Gains and losses of intertidal habitat outside of the site (and the carbon stored in those habitats) that are a direct result of the restoration should be considered	Not considered in this study.	A five year monitoring programme for the scheme found no evidence that the scheme had caused increased erosion in the main estuary channel bed [70]. Near to the scheme, the most significant changes have been associated with the erosion of the exit channel due to the strong flows into and out of the realignment site [31]. Erosion in the exit channel has progressed into the site through the creation of a distinct step, and these changes within the site are captured in our analysis.
Carbon in sediment gained	Cores taken at 11 locations in the restored site, average carbon content of new sediment used.	We found total carbon and total organic carbon in new sediment was somewhat lower than in the adjacent natural saltmarsh. The site was in the early stages of restoration (first 4 y). Further development of biotic communities, particularly the vegetation, may increase the carbon content of the sediment at the restored site. Some spatial variation in carbon contents of new sediment around the site. Reasons for this were not clear but understanding this

		would allow more spatially refined models of carbon accumulation could be made.
Carbon in sediment lost (eroded)	Assumed to be the same as carbon gained.	Carbon content of the soils eroded (e.g. from main creek) is likely to be lower than that in the new sediment because the agricultural soils significantly had lower carbon. However, this could not be quantified because erosion in the main creek was up to 5 m deep. Some of the erosion later in the study would have been of newly accreted sediments (e.g. due to formation of small creeks) and thus of same carbon content as that gained. In total, this approach has likely underestimated total carbon gained.
Source of carbon in sediment	Not considered	Burial of <i>in situ</i> derived carbon would be a true gain. Carbon from outside the site may have ended up being stored elsewhere in the absence of the site, or may have been oxidised; the extent to which either happens is uncertain. The total carbon accumulation here provides an upper bound for net carbon buried.
Plant biomass	Not considered	Belowground biomass contributes to carbon accumulation, and is expected to increase as the site became more vegetated. Similarly, more vegetation creates a source of carbon to be buried.
Greenhouse gas fluxes	Not considered	Release of greenhouse gases (e.g. methane) may offset some carbon accumulation. Burden <i>et al.</i> [69] found CH ₄ and N ₂ O fluxes were close to zero on a restored and natural saltmarsh in Essex. However, Adams, Andrew & Jickells [71] suggest gas fluxes

		could reduce carbon sequestration on MR sites by 24%.
Construction carbon costs	Calculated using estimated fuel use during construction in combination with estimates from the Environment Agency's basic carbon calculator (version 3.1.2) for personnel travel, energy use in portable accommodation, and the embodied emissions associated with construction materials.	<p>Creation of the embankments is very likely to be the greatest construction carbon cost of the managed realignment, and itself is small compared to the carbon gained by the habitat created on the site.</p> <p>All material for the managed realignment part of the site were locally-won material for the embankments from borrow pits on site and was not imported.</p> <p>Since the completion of the Steart project, a more up-to-date Environment Agency carbon estimation tool became available, which considers the carbon of other project stages (operational, decommissioning) to provide the whole-life carbon over a 100-years. The tool currently cannot be adjusted to deal with locally-won embankment material, and was not used here.</p> <p>Some operational carbon cost will occur from the site managers WWT, but has not been included in the calculations. This would include activities associated with site inspections and the maintenance of the embankments (such as grazing by sheep rather than mowing). It is expected to be minimal compared with construction. No decommissioning is anticipated.</p>
Prior land use – some changes in land use may result in substantial carbon lost, e.g. loss of trees	Not considered	The site was a mix of arable and pasture prior to restoration and relatively few trees were removed during construction, but this should be considered for future sites.

739 **SUPPLEMENTARY INFORMATION**

740

741 **Table S1.** Field sampling dates and information. Samples highlighted in bold are those selected for
742 the quantification of total organic carbon. Access issues prevented sampling at some locations in
743 March 2015 and September 2016. We assessed the consequence of the additional uneven sampling
744 by removing samples from these two time periods and recalculating the mean carbon content in
745 newly accreted sediment. The value differed by less than 1% of the original value (i.e. 4.367% vs
746 4.372%), so we retain all samples in the data presented in the manuscript.

Date of sampling	Days after restoration	Cores sampled	Notes
28 August 2014	-7	Site A1, A2 Site B1, B2 Site C1, C2, C3 Site D1, D2, D3	Pre-restoration sampling. Natural marsh not sampled. A3 not sampled as it was undergoing earthworks.
14-15 December 2014	+101	Site A1, A2, A3 Site B1, B2 Site C1, C2, C3 Site D1, D2, D3 NAT	Installation of sedimentation pins
16-17 March 2015	+193	Site A2 Site C1, C2, C3 Site D1, D2, D3 NAT	Access issues prevented sampling at Site B, A1 and A3.
25-28 June 2015	+294	Site A1, A2, A3 Site B1, B2 Site C1, C2, C3 Site D1, D2, D3 NAT	
14-15 April 2016	+588	Site A1, A2, A3 Site B1, B2 Site C1, C2, C3 Site D1, D2, D3 NAT	
27-28 September 2016	+754	Site B1, B2 Site C1, C2 Site D1, D2, D3	Access issues prevented sampling at Site A and C3.
5-7 March 2017	+913	Site A1, A2, A3 Site B1, B2 Site C1, C2, C3 Site D1, D2 , D3	Sedimentation pin data collected

747

748 **Table S2.** Summary of the fuel (diesel) consumption and tCO₂e emitted by machinery in the
749 construction of Steart Marshes earthworks.

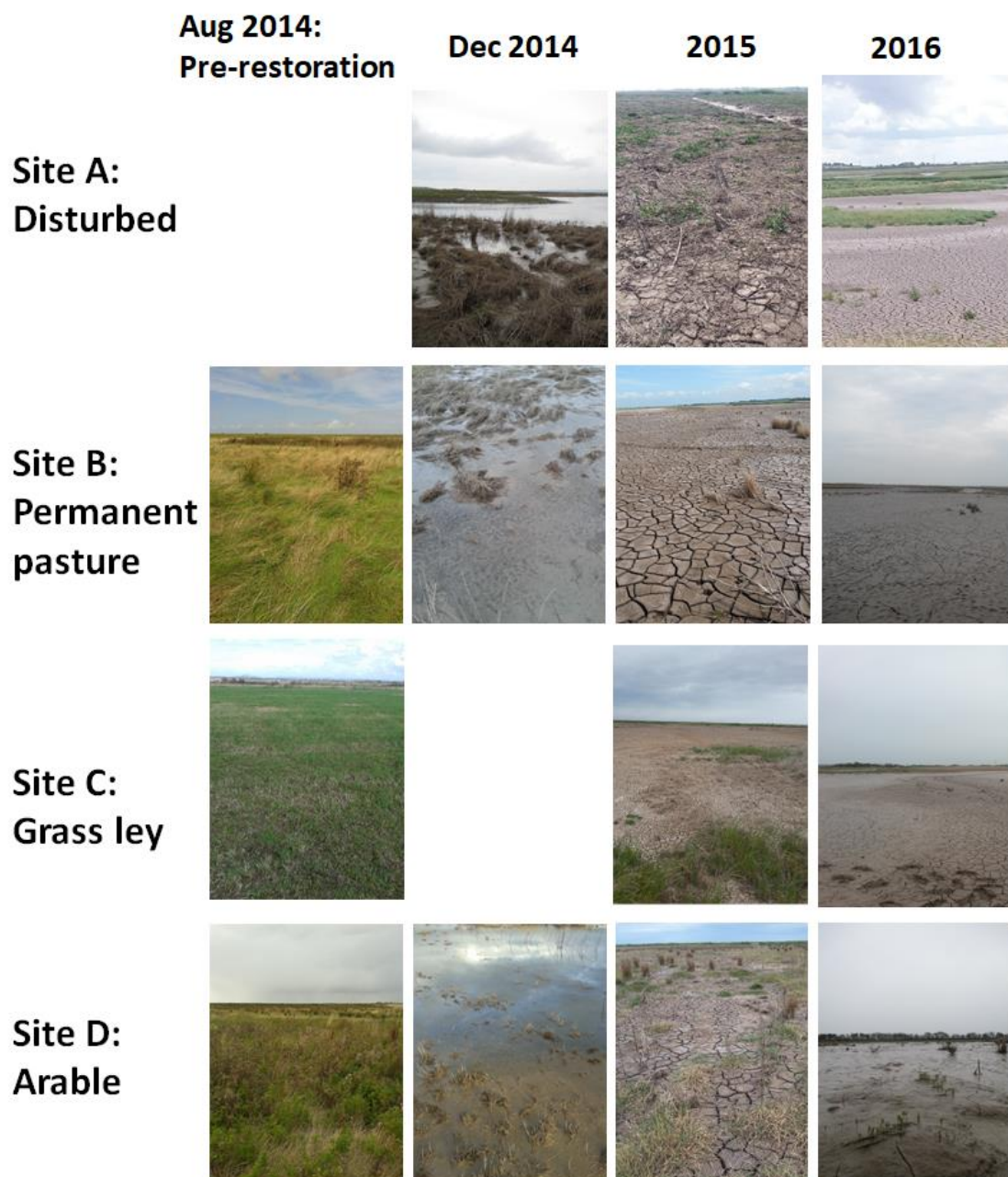
Equipment/Component	Average fuel burn (l.hr ⁻¹)	Productivity	Fuel use (l)	t CO ₂	tC
Excavator (EC250DL)	20.8 ²	80m ³ /hr ⁶	127,255	341.0	93.0
A25D ADT	30 ¹	10 km/hr ⁵	208,689	559.3	152.5
D6 Bulldozer	19 ³	45.7m ³ /hr ⁷	203,488	545.3	148.7
Roller	1.9 ⁴		11,580	31.0	8.5
Managed Realignment Earthworks			551,012	1,476.7	402.7
Other Earthworks			110,202	295.3	80.5
Total Earthworks			661,214	1,772	483

750 ¹<https://www.equipmentworld.com/owning-and-operating-costs-5>; ²<https://www.volvoce.com/en-us/government/services/promotions/fuel-efficiency-guarantee>; ³<https://www.constructionequipmentguide.com/industry-begins-grappling-with-rising-fuel-costs/7008>; ⁴<https://www.equipmentworld.com/owning-and-operating-costs-6/>; ⁵
751 Estimated from average speed on site (obtained from the contractor); ⁶ Hydraulic Excavator with a 0.5 m³ bucket
752 excavating clay/chalk, [https://www.methvin.org/construction-production-rates/excavation/bulk-](https://www.methvin.org/construction-production-rates/excavation/bulk-excavation)
753 bucket, reach of 50-200 m², Boulder Clay <https://www.methvin.org/construction-production-rates/excavation/bulk->
754 excavation
755
756

757

758

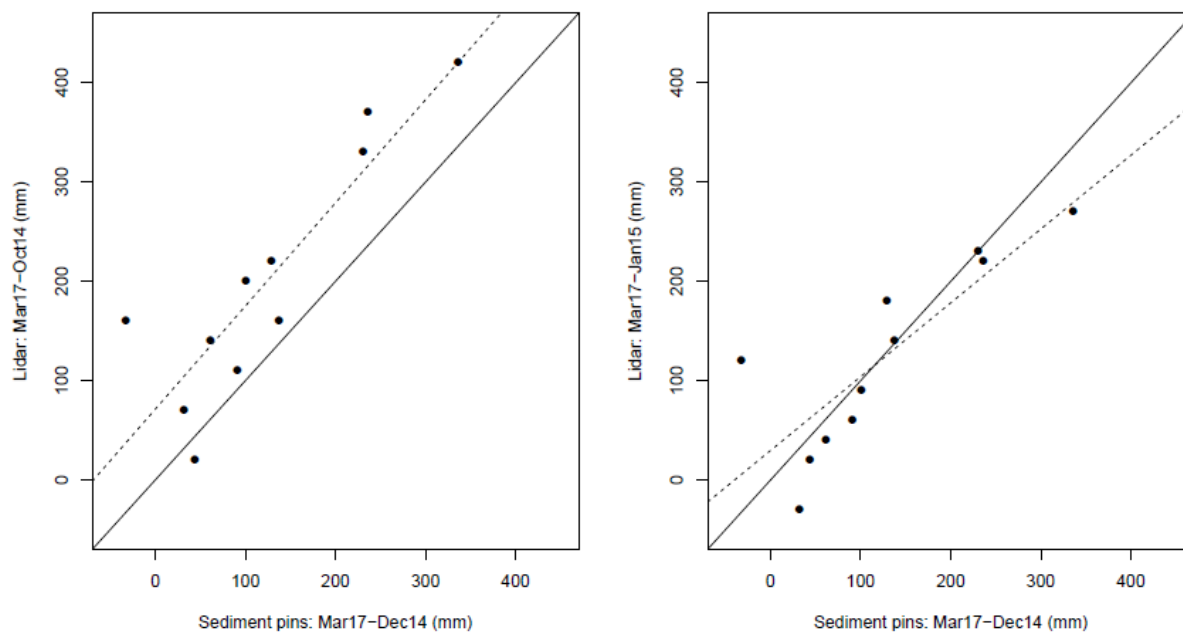
759



760

761 **Figure S1.** Photographs of sampling areas (Sites A-D).

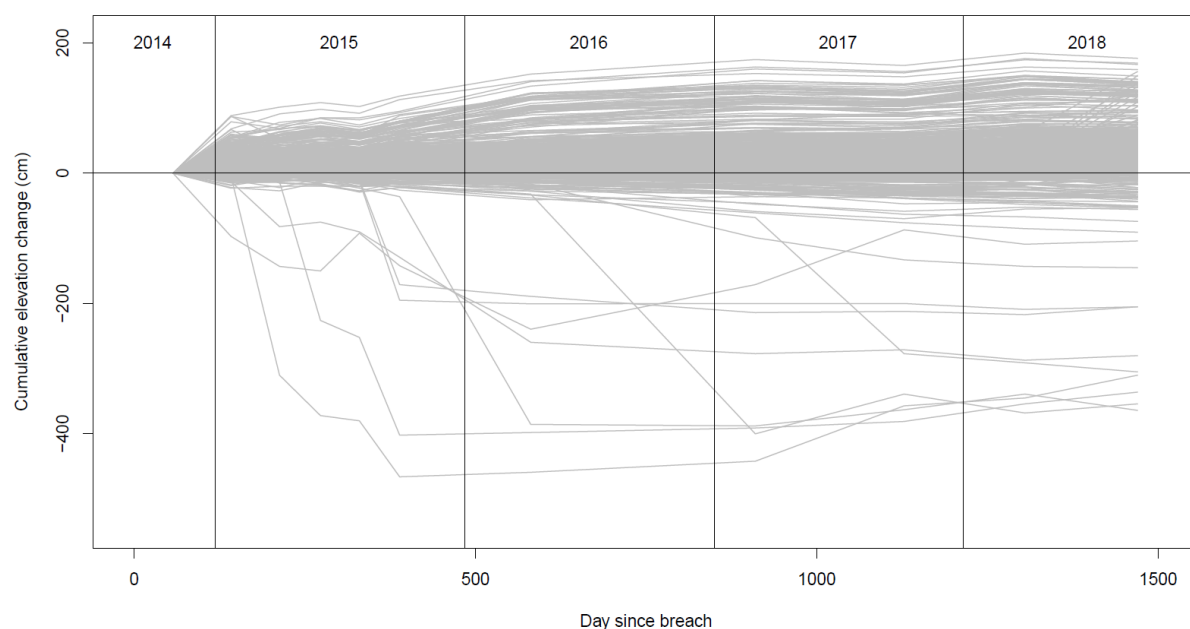
762



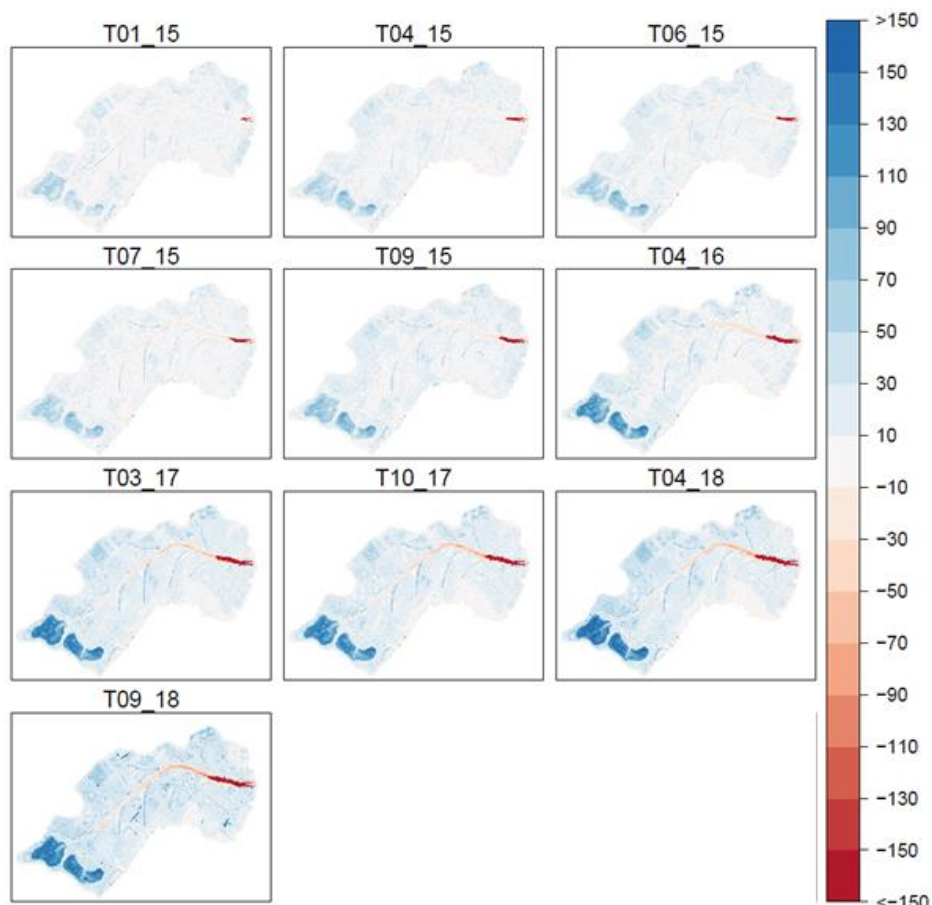
763
764 **Figure S2.** Relationship between elevation change measured with LiDAR derived-DTMs and in situ
765 measurements with pins. In situ measured data (x axis) show difference in elevation between
766 December 2014 (3 months after restoration) and March 2017. Left: Compares in situ data to
767 elevation changes derived from LiDAR data taken in October 2014 and March 2017, and Right
768 compares elevation changes between January 2015 and March 2017. No LiDAR images are available
769 for December 2014. Solid lines show a 1:1 relationship and the dashed lines show the actual
770 relationship (linear regression) between DTM-derived and in situ measurements (Left: $R^2 =$
771 0.775, $P < 0.001$; Right $R^2 = 0.686$, $P = 0.002$). LiDAR measurements are strongly related to in situ
772 measurements and are not systematically biased when sampling periods are more closely matched
773 (i.e. Right).

774

775
776
777



778
779 **Figure S3.** Cumulative elevation change trajectories of a sample of 1000 DTM pixels.
780



781
782

Figure S4. Cumulative change in elevation for each LiDAR survey.

783